Journal of Catalysis 311 (2014) 314–324

Contents lists available at ScienceDirect

Journal of Catalysis

journal homepage: www.elsevier.com/locate/jcat

Remarkable enhancement of dichloromethane oxidation over potassium-promoted Pt/Al_2O_3 catalysts

Yu Wang, Huan-Huan Liu, Shu-Yuan Wang, Meng-Fei Luo, Ji-Qing Lu *

Key Laboratory of the Ministry of Education for Advanced Catalysis Materials, Institute of Physical Chemistry, Zhejiang Normal University, Jinhua 321004, China

ARTICLE INFO

Article history:
Received 19 November 2013
Revised 23 December 2013
Accepted 30 December 2013
Available online 28 January 2014

Keywords:
Dichloromethane oxidation
Potassium promotion
Pt/Al_2O_3 catalysts
Reducibility
Formate species

ABSTRACT

A series of K-promoted Pt/Al_2O_3 catalysts were prepared by an incipient wetness impregnation method and tested for oxidation of dichloromethane (DCM). It was found that the activity was greatly enhanced by the modification of K, which depended on the K content in the catalyst. The T_{50} temperature on a 0.42K–2Pt/Al_2O_3 catalyst was 270 °C, which was much lower than that on a K-free 2Pt/Al_2O_3 catalyst (400 °C). The remarkable improvement of activity was attributed to the enhanced catalyst reducibility, by the generation of Pt–O–K_x ($x \approx 2$) surface species through an intimate interaction between K and Pt. The presence of such Pt–O–K_x species in the catalyst could significantly accelerate the decomposition of formate intermediates formed on Al_2O_3 surface and thus the overall reaction, as evidenced by the in situ Fourier transform infrared spectroscopic results.

1. Introduction

The abatement of chlorinated volatile organic compounds (CVOCs) such as dichloromethane (DCM), 1,2-dichloroethane (DCE) and trichloroethylene (TCE) becomes a very important topic because these compounds are recognized as major pollutants which are hazardous to the environment and public health [1]. Among all the technologies for CVOCs elimination, catalytic oxidation is considered as a promising one and thus has been widely studied, due to its high catalytic performance for the destruction of low-concentration contaminants, high selectivity to harmless intermediates, and less severe operation conditions [2]. The employed catalysts for CVOCs oxidation mainly include noble metals [3–7], transition metal oxides [8–14] and zeolites [15–19]. Despite of the disadvantages such as chlorine poisoning and thus catalyst deactivation [20], noble metal catalysts such as Pt and Pd are usually more active than the oxides and thus they have received much attention.

Continuous efforts have been made to develop effective catalysts for CVOCs oxidation. It is believed that the performance of the catalyst is usually determined by several key factors such as surface acidity and redox properties [17,21,22], as the former is important for chemisorption of CVOC molecules and the latter is important for oxygen activation. Therefore, one reasonable approach is the improvement of catalyst reducibility. In this case, CeO_2 seems to be a good choice because of its remarkable redox capability which could significantly ease the activation of oxygen during the oxidation reaction [23,24]. For example, CeO_2-modified oxide catalysts such as CeO_2–ZrO_2 [21,22], CeO_2–MnO_x [25] and CeO_2–Cr_2O_3 [26] were more active for CVOCs oxidation than their mono-metal counterpart, due to the enhanced reducibility with the presence of CeO_2 in the catalysts. Such strategy could also be applied to other catalyst systems. Zhang et al. [27] studied A-site substituted $LaMnO_3$ perovskite catalysts with Sr, Mg and Ce for vinyl chloride oxidation, and they found that the Ce-substituted $La_{0.8}Ce_{0.2}MnO_3$ had the highest activity, which was due to its high surface area and low-temperature reducibility. Pt/Al_2O_3 catalysts are also widely used for VOCs oxidation [28–30] and the improvement of the catalytic performance on these Pt catalysts has been investigated. For example, in our recent work [31], we reported CH_2Cl_2 oxidation over Pt/Al_2O_3 catalysts and it was found that the modification of Pt/Al_2O_3 catalysts with CeO_2 significantly improved the catalyst reducibility, which was helpful to the enhancement of the catalytic activity. Similar promoting effects of CeO_2 were also observed on Pt/Al_2O_3 catalysts for total oxidation of toluene, benzene, and xylene [32].

Since highly efficient catalyst systems are always desirable, new approaches of catalyst promotion are necessary. It was reported in literature that alkali-promoted Pt catalysts exhibited improved activities in various reactions, such as preferential CO oxidation (PROX) [33–35], water–gas-shift reaction [36–38] and low-temperature oxidation of formaldehyde [39]. In PROX over Pt/Al_2O_3 catalysts, the addition of K weakened the interaction between CO and Pt and also changed the CO adsorption site [33].

* Corresponding author. Fax: +86 579 2282595.
E-mail address: Jiqinglu@zjnu.cn (J.-Q. Lu).

0021-9517/$ - see front matter © 2014 Elsevier Inc. All rights reserved.
http://dx.doi.org/10.1016/j.jcat.2013.12.018

In water–gas-shift reaction, alkali-stabilized Pt–OH_x species in Na- or K-promoted Pt/Al_2O_3 and Pt/SiO_2 catalysts were proposed to explain the reaction at low temperature [37]. Also, the reaction pathway may alter upon the addition of alkali ions, as evidenced in HCHO oxidation over alkali metal-promoted Pt/TiO_2 and Pt/SiO_2 catalysts [39].

Inspired by the findings in literature mentioned above and as a continued study of our previous work [31], in this paper, we report our investigations of CH_2Cl_2 oxidation over a series of potassium-promoted Pt/Al_2O_3 catalysts. It turned out that the modification of K could greatly enhance the activities, which was closely related to the changes in the catalyst properties by the K-promotion.

2. Experimental

2.1. Catalyst preparation

K-Pt/Al_2O_3 catalysts were prepared by an incipient wetness impregnation method. The γ-Al_2O_3 support (S_{BET} = 180 $m^2\ g^{-1}$) was calcined 500 °C for 4 h prior to use. In a typical preparation, the γ-Al_2O_3 support was added to a mixed aqueous solution of H_2PtCl_6 and KNO_3 (with a K/Pt weight ratio of 1/2) with proper volume and impregnated for 4 h. After that, the mixture was dried at 120 °C overnight and calcined in air at 500 °C for 4 h. Then, the samples were washed with deionized water at room temperature for three times, then filtered and dried at 120 °C overnight. The K-free Pt/Al_2O_3 catalysts were prepared in a similar manner but without the addition of K in the process. The resulting catalysts were designated as xK–yPt/Al_2O_3, where x and y refer to the contents (wt.%) of K and Pt in the catalyst, respectively.

2.2. Characterizations

Actual contents of Pt and K in the catalysts were determined by inductively coupled plasma-atomic emission spectrometry measurements (ICP-AES, Optima 7300DV, Perkin Elmer).

The BET surface areas of the catalysts were measured by N_2 adsorption at liquid-nitrogen temperature (77 K), using a surface area analyzer (Quantachrome Autosorb-1). The catalysts were pretreated at 120 °C for 6 h in vacuum.

X-ray diffraction (XRD) patterns were recorded with a PANalytical ẊPert PRO MPD powder diffractometer using Cu Kα radiation. The working voltage was 40 kV and the working current was 40 mA. The patterns were collected in a 2θ range from 10° to 80°, with a scanning speed of 0.15° s^{-1}.

High-resolution transmission electron microscopy (HRTEM) was performed on a JEM-2100F microscopy with a field emissive gun, operated at 200 kV and with a point resolution of 0.24 nm.

Hydrogen temperature-programed reduction (H_2-TPR) technique was employed to analyze the reducibility of the catalyst. 25 mg of the catalyst was placed in a quartz reactor and pretreated in a O_2 flow (20 ml min^{-1}) at 300 °C for 60 min in order to remove the adsorbed water and carbonates and then the sample was cooled down to 50 °C in a He flow (20 ml min^{-1}). After that, the sample was heated from 50 to 800 °C with a heating rate of 10 °C min^{-1} under a mixture of 5% H_2-95% N_2 (20 ml min^{-1}). The amount of H_2 consumption was determined by a gas chromatograph with a thermal conductivity detector (TCD).

The surface acidity of the catalyst was measured by ammonia temperature-programed desorption (NH_3-TPD). 50 mg of the catalyst was pretreated in a flow of N_2 (20 ml min^{-1}) at 300 °C for 0.5 h and then was cooled down to 50 °C. Afterward, a NH_3 flow (20 ml min^{-1}) was introduced to the sample for 15 min, followed by purging at 80 °C for 0.5 h with a N_2 flow (20 ml min^{-1}) to remove the physisorbed NH_3. Then, the sample was heated from 80 to 800 °C at a rate of 10 °C min^{-1}, and the profile was recorded using a gas chromatograph (TECHTEMP GC 7890II) with a TCD detector.

Dispersion of Pt in the catalyst was determined by CO chemisorption, which was carried out on a Quantachrame CHEMBET-3000 instrument. The sample was placed in a quartz U-tube, and high-purity He (99.999%) was used as the carrier gas. The sample was reduced in a H_2–N_2 mixture stream (5 vol% H_2, 30 ml min^{-1}) at 300 °C for 1 h and cooled down to 30 °C in a pure He flow. Then, pulses of CO were fed into the stream of carrier gas with a precision analytical syringe. The dispersion was calculated based on the assumption that CO/surface Pt atom = 1. And, the Pt particle size was calculated based on the equation d_{Pt} (nm) = 1.1/D (D = dispersion).

X-ray photoelectron spectra of the catalysts were obtained on an ESCALAB 250Xi instrument, with a Al Kα X-ray source (1486.6 eV), under about 2×10^{-9} mbar at room temperature and a pass energy of 20 eV. The binding energy (BE) of C1s core level at 284.6 eV was taken as an internal standard.

Temperature-programed surface reaction was conducted on a home-made reactor connected with a mass spectrometer (MS, Qic-20 Benchtop, HidenAnalytical). 50 mg of the catalyst was pretreated in a flow of O_2 (20 ml min^{-1}) at 300 °C for 0.5 h and then was cooled down to 30 °C. Then, a flow of CH_2Cl_2/O_2 mixture (3000 ppm CH_2Cl_2, total flow rate = 20 ml min^{-1}) was introduced to the reactor and the sample was heated from 30 to 500 °C at a rate of 10 °C min^{-1}. And, m/e signals of 28, 44, 18, 36.5, 50.5, 85, and 30 were monitored, corresponding to CO, CO_2, H_2O, HCl, CH_3Cl, CH_2Cl_2, and HCHO, respectively.

In situ Fourier transform infrared (FTIR) spectra of the samples were recorded on a NEXUS670 spectrometer equipped with a MCT detector. Self-supported sample wafers (diameter = 16 mm) were prepared from 30 mg of sample by pressing at about 3 MPa. The sample was transferred to a quartz IR cell connected to the closed circulation systems and then pretreated under an air flow (90 ml min^{-1}) at 400 °C for 1 h. After the pretreatment, the sample was cooled down to 30 °C and 1 ml of a gas mixture (3000 ppm CH_2Cl_2 in air) was introduced to the IR cell and the sample was heated from 30 to 400 °C at a ramp of 10 °C min^{-1}. Temperature-dependent FTIR spectra during the reaction were recorded after holding each temperature point for 10 min.

2.3. Activity test

Catalytic combustion of CH_2Cl_2 was carried out in a conventional fixed-bed reactor (i.d. = 9 mm). 1.0 g of the catalyst in 40–60 mesh was diluted into a volume of 2 ml with quartz sand, and then, it was loaded in the reactor. A thermal couple was placed in the middle of the catalyst bed to monitor the reaction temperature. The catalyst was then heated from r.t. to desired temperature at a heating rate of 10 °C min^{-1} in air (50 ml min^{-1}). When the desired temperature was reached, the air was stopped and a gaseous mixture of CH_2Cl_2 and moisture-containing air was introduced to the catalyst, and the concentration of CH_2Cl_2 was 3000 ppm (total flow rate = 500 ml min^{-1}, GHSV = 15 000 h^{-1}). After holding certain reaction temperature for 1 h (to stabilize the reaction), analyses of the products were conducted. The concentrations of CH_2Cl_2 and other organic products during the reaction were analyzed by a gas chromatograph (Shimadzu, GC-14C) equipped with a FID detector. Also, in order to avoid possible corrosion of the GC system by produced HCl or Cl_2, the outlet reaction mixture was neutralized by passing through a 0.1 M NaOH aqueous solution.

Conversion of CH_2Cl_2 was calculated as follows:

$$X_{CH_2Cl_2} = \frac{[CH_2Cl_2]_{in}\text{vol.}\% - [CH_2Cl_2]_{out}\text{vol.}\%}{[CH_2Cl_2]_{in}\text{vol.}\%}$$

where $[CH_2Cl_2]_{in}$ and $[CH_2Cl_2]_{out}$ were the CH_2Cl_2 concentrations in the inlet and outlet gas (vol.%) respectively.

The kinetic study was performed on the same fixed-bed reactor of the catalytic CH_2Cl_2 oxidation as mentioned above. The feed gases were measured with mass flow controllers and mixed prior to the reactor inlet. For kinetic measurements, the reactor was operated in a differential mode with the CH_2Cl_2 conversion less than 15%. 0.5 g catalyst in 40–60 mesh was diluted with quartz sand to a volume of 2 ml and the reaction conditions were the same as in the above-mentioned fixed-bed testing. Also, the absence of mass transport resistances was checked by Weisz–Prater criterion for internal diffusion and Mears' criterion for external diffusion and the absence of heat transfer was checked by Mears' criterion [40] (see Supplementary information for detailed calculation). For example, on a 0.42K–2Pt/Al_2O_3 catalyst, the calculated values under kinetic conditions are 1.47×10^{-2} for the Weisz–Prater criterion for internal diffusion, 1.19×10^{-2} for the Mears' criterion for external diffusion and 0.034 for the Mears' criterion for heat transfer. Those results ensure plug-flow and isothermal conditions within the catalyst bed.

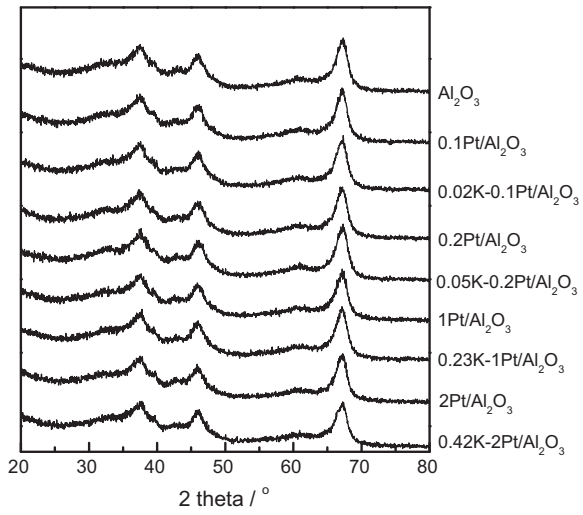

Fig. 1. XRD patterns of Pt/Al_2O_3 catalysts.

3. Results

3.1. Physical properties

Table 1 summarizes physical properties of the catalysts. The BET surface areas of the catalysts range from 166 to 180 $m^2\ g^{-1}$, which are similar to that of the Al_2O_3 support because of the low contents of K and Pt in the catalysts. The contents of Pt in the catalysts are close to the nominal values in the preparation process, but the contents of K are much lower compared to the nominal values because main part of the potassium salts could be dissolved in H_2O and removed in the washing procedure during the preparation. In addition, the resulting K loading in the catalyst is related to the Pt content, with a K/Pt molar ratio close to 1. Pt dispersions in the catalysts measured by CO chemisorption reveal that for the K-free samples, the Pt dispersions slightly decline with increasing Pt content, with a value of 56.1% on the 0.1Pt/Al_2O_3 and 44.0% on the 2Pt/Al_2O_3. The decline in Pt dispersion is due to the aggregation of small Pt particles in the high-content samples, and consequently the Pt particle size increases. With the addition of K, it is found that the Pt dispersion is generally slightly higher compared to the corresponding K-free counterpart. For example, the 0.42K–2Pt/Al_2O_3 catalyst has a Pt dispersion of 56%, which is higher than that of the 2Pt/Al_2O_3 (44%) and thus suggests that the presence of K helps in the dispersion of Pt species in the catalyst.

Fig. 1 presents the XRD patterns of the catalysts. The patterns of the catalysts are identical to that of the Al_2O_3 support and no diffraction peaks of Pt and K are observed. This is due to the fact that the loadings of the metal species in the catalysts are low and these species are highly dispersed on the catalyst surface thus under the detection limit of XRD technique. Also, as the most intense diffraction peaks of Pt species are located in 2θ range of 27–40° (PDF 04-0802 for Pt^0; PDF 42-0866 and 47-1171 for PtO; PDF 43-1045, 38-1355, 37-1087 and 23-1306 for PtO_2), amplified XRD patterns of the samples in this range are checked (See Fig. S1 in Supplementary information). No distinct diffraction peaks of any Pt species (Pt^0, PtO and PtO_2) could be found. Thus, the XRD results are in good agreement with the Pt particle sizes measured by CO chemisorption (about 2.0–2.5 nm, Table 1) because metal particle sizes less than 3 nm could not be detected by XRD.

Representative TEM images of some prepared samples are presented in Fig. 2. The existence of Pt species is confirmed by measuring the d-space distance of the particles. The detected Pt particle sizes in these samples are 3–4 nm, which are larger than the values obtained by CO chemisorption (Table 1), probably due to the fact that the particle size calculated by CO chemisorption is an average value.

3.2. Redox properties

Redox properties of the catalysts were measured by H_2-TPR technique, as shown in Fig. 3. In Fig. 3a, the Al_2O_3 support does not show any distinct reduction peak in the temperature range of 50–700 °C. With the addition of small amount of Pt (0.1% and 0.2%), a weak reduction peak (β_1) is observed at about 500 °C, which could be assigned to the reduction of two dimensional dispersive oxychlorinated platinum [41].

And this reduction peak becomes more intense with increasing Pt content in the catalyst. For the high-loading samples

Table 1
Physical properties of Pt/Al_2O_3 catalysts.

Catalyst	S_{BET}/$m^2\ g^{-1}$	Metal content/wt.%		K/Pt molar ratio	Metal dispersion/%	Pt particle size/nm	TOF[a]/$\times 10^{-2}\ s^{-1}$
		Pt	K				
0.1Pt/Al_2O_3	180	0.15	–	–	56.1	2.0	6.05
0.02K–0.1Pt/Al_2O_3	176	0.10	0.02	1.00	54.2	2.0	10.8
0.2Pt/Al_2O_3	171	0.24	–	–	54.3	2.0	4.17
0.05K–0.2Pt/Al_2O_3	173	0.23	0.05	1.25	55.6	2.0	7.38
1Pt/Al_2O_3	174	1.15	–	–	47.0	2.5	0.92
0.23K–1Pt/Al_2O_3	173	0.85	0.06	0.98	52.8	2.1	4.42
2Pt/Al_2O_3	175	2.08	–	–	44.0	2.5	0.37
0.42K–2Pt/Al_2O_3	166	2.15	0.42	0.98	56.0	2.0	1.81

[a] CH_2Cl_2 conversions were taken at reaction temperature of 350 °C in Fig. 7.

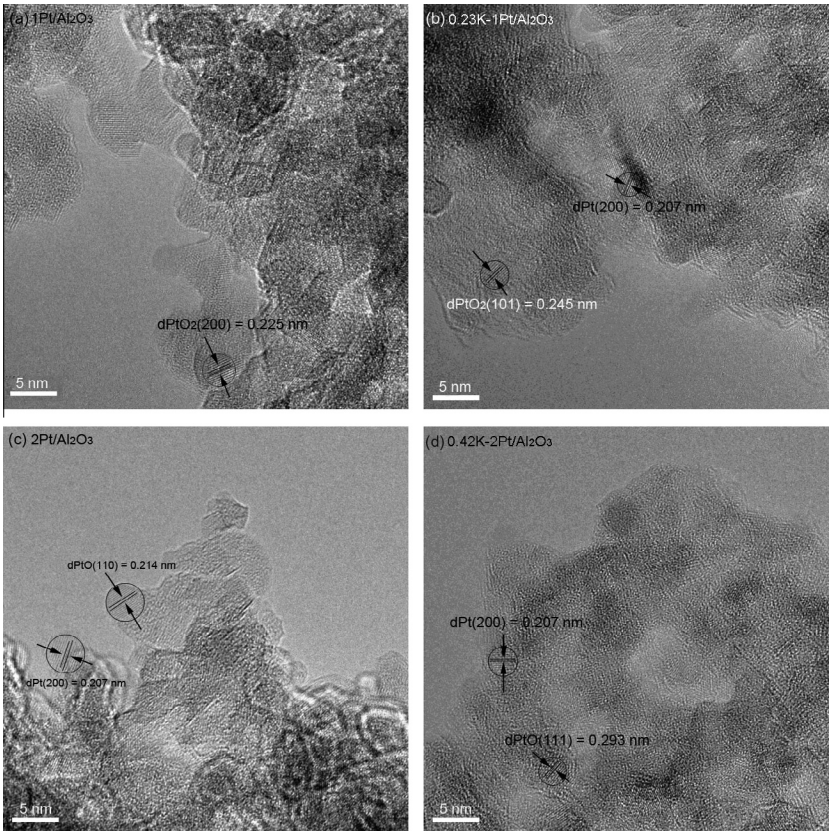

Fig. 2. TEM images of (a) $1Pt/Al_2O_3$, (b) $0.23K–1Pt/Al_2O_3$, (c) $2Pt/Al_2O_3$ and (d) $0.42K–2Pt/Al_2O_3$ catalysts.

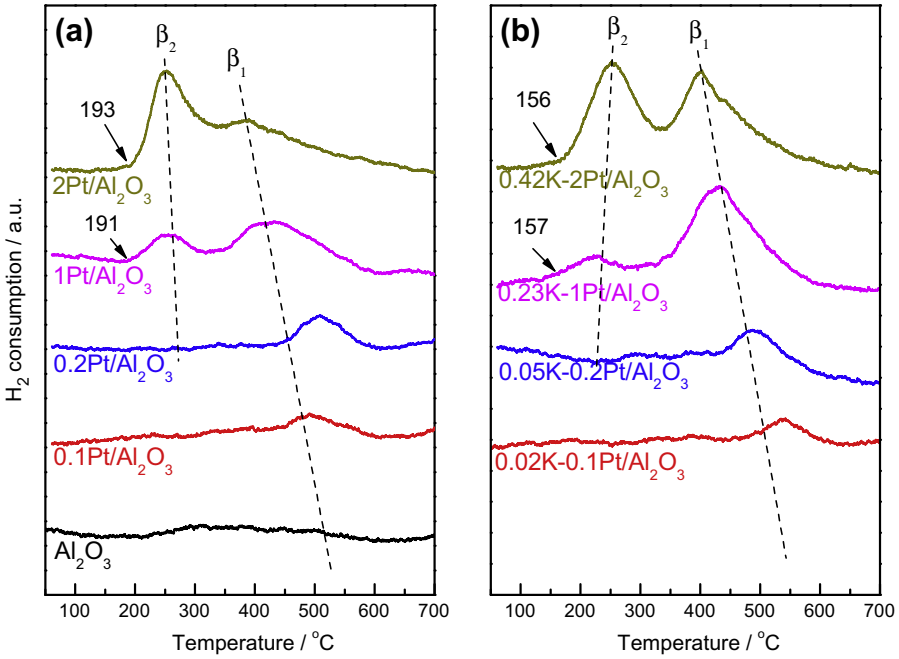

Fig. 3. H_2-TPR profiles of (a) Pt/Al_2O_3 and (b) K-promoted Pt/Al_2O_3 catalysts.

(Pt contents of 1.0% and 2.0%), additional low-temperature reduction peaks (β_2) centered at 200–250 °C are observed, which could be assigned to the reduction of dimensional bulk phase of oxy- or hydroxychlorinated platinum [41]. The absence of the β_2 peak in the low Pt-content samples (0.1% and 0.2%) may lie in the fact that in these samples the Pt species are highly dispersed on Al_2O_3 surface due to the very low loadings. The area of the β_2 peak also increases with Pt content in the catalyst. Meanwhile, the position of the β_1 peak gradually shifts to lower temperature with increasing Pt contents in the catalysts, probably due to a

spillover effect. The K-promoted samples have similar reduction properties compared to their K-free counterparts (Fig. 3b), but distinct difference is still observed. For example, the low-temperature reduction peak (β_2) starts at much lower temperature on the K-containing sample (at about 156 °C) compared to the K-free sample (at about 190 °C). The shift to lower reduction temperature for the K-promoted catalyst could be related to two facts. One is that the addition of K leads to smaller Pt particles in the catalyst, as the dispersions of Pt in the K-promoted samples (0.23K–1Pt/Al_2O_3 and 0.42K–2Pt/Al_2O_3) are higher than those of the corresponding K-free ones (Table 1), which makes the Pt species in the K-promoted sample more reducible. The other is that the K-promotion may cause the evolution of new surface species which could be easily reduced [37]. Nevertheless, the H_2-TPR results indicate that the K-promotion significantly enhances the reducibility of the Pt catalysts, particularly at low-temperature region.

3.3. Surface acidity

Surface acidities of the catalysts were measured by NH_3-TPD, and the results are shown in Fig. 4. All the samples show a broad desorption peak centered at about 210 °C, which could be assigned to NH_3 desorbed from Lewis acid sites in Al_2O_3 [42]. For the Pt/Al_2O_3 catalysts (Fig. 4a), it is found that the relative amount of surface acidic sites gradually increases with increasing Pt content especially for the 1Pt/Al_2O_3 and 2Pt/Al_2O_3 samples, due to the introduction of residual chlorine species in the catalyst as the H_2PtCl_6 was used as the precursor. In contrast, the surface acidity does not change much on the K-promoted catalysts (Fig. 4b). Moreover, compared to the corresponding Pt/Al_2O_3 catalyst, the addition of K in the catalyst remarkably reduces the surface acidity. For example, the 2Pt/Al_2O_3 catalyst has a relative amount of surface acidic sites of 4.08, while the amount obtained on the 0.42K–2Pt/Al_2O_3 is 1.24. The suppression of surface acidity in the K-promoted samples could be attributed to two facts. On one hand, during the catalyst preparation, K cations could react with residual Cl anions to form KCl, which could be dissolved in H_2O in the washing process. On the other hand, the presence of potassium oxides could possibly block some acidic sites on the catalyst and consequently reduce the surface acidity.

3.4. Analysis of oxidation states and surface compositions

The oxidation states of the catalysts were analyzed by XPS and the results are shown in Fig. 5 and Table 2. Since the Al 2p line overlaps with the Pt 4f one, the Pt 4d line was used in the study. Also, because of the low Pt contents in the 0.1Pt/Al_2O_3 and 0.2Pt/Al_2O_3 catalysts and low intensity of Pt 4d XPS signals, only those with relatively high Pt contents (1Pt/Al_2O_3 and 2Pt/Al_2O_3) were measured. As shown in Fig. 5a, a broad band (310–322 eV) is observed in all samples, which could be further deconvoluted into three components with binding energies (BEs) at 313.6–314.2, 316.2–316.3, and 318.7–319.2 eV (Table 2). The first component could be assigned to metallic Pt (Pt^0) [43]. The BE at 316.2–316.3 eV is typical for PtO species [44]. The BE values at 318.7–319.2 eV are higher compared to that of pure PtO_2 [45], which would be related to some incompletely decomposed Pt–Cl-containing species ($[Pt^{IV}O_xCl_y]_s$) formed by the interaction between Pt and Cl due to the use of H_2PtCl_6 precursor [46]. Results in Table 2 also reveal that oxidized Pt species are dominant in these catalysts. Moreover, it is found in Table 2 that the proportion of oxidized Pt species (Pt^{2+} and Pt^{4+}) in the K-promoted sample is higher than that in the corresponding K-free one, suggesting more reducible Pt species in the K-promoted sample. As for the O 1s spectra (Fig. 5b), the broad peak could be deconvoluted to two peaks at 530.3–530.9 and 531.8–532.6 eV, which could be assigned to lattice oxygen species (O^{2-}_{latt}) and absorbed oxygen species or surface hydroxyl groups (O_{ads}) [47], respectively. And, the surface contents of these two oxygen species are almost equal.

3.5. Catalytic performance

First of all, product distributions over the catalysts were investigated and the results are shown in Fig. 6. In general, no signals of any products are detected at low temperature (<300 °C) on all the samples, and the signal of reactant (CH_2Cl_2) also remains unchanged because its concentration in the feedstock is constant since no reaction occurs at low-temperature region. At elevated temperature (>300 °C), signals of various products emerge, accompanied by slight decrease in CH_2Cl_2 concentration (negative peak) indicating that CH_2Cl_2 is consumed. On the Al_2O_3 support (Fig. 5a), the main products detected are CO, CO_2, CH_3Cl, H_2O and

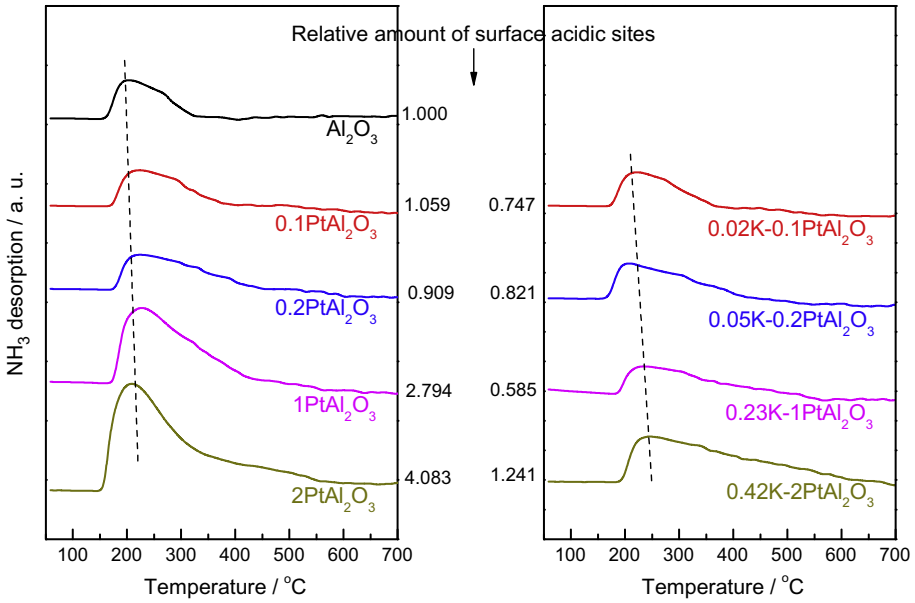

Fig. 4. NH_3-TPD profiles of (a) Pt/Al_2O_3 and (b) K-promoted Pt/Al_2O_3 catalysts.

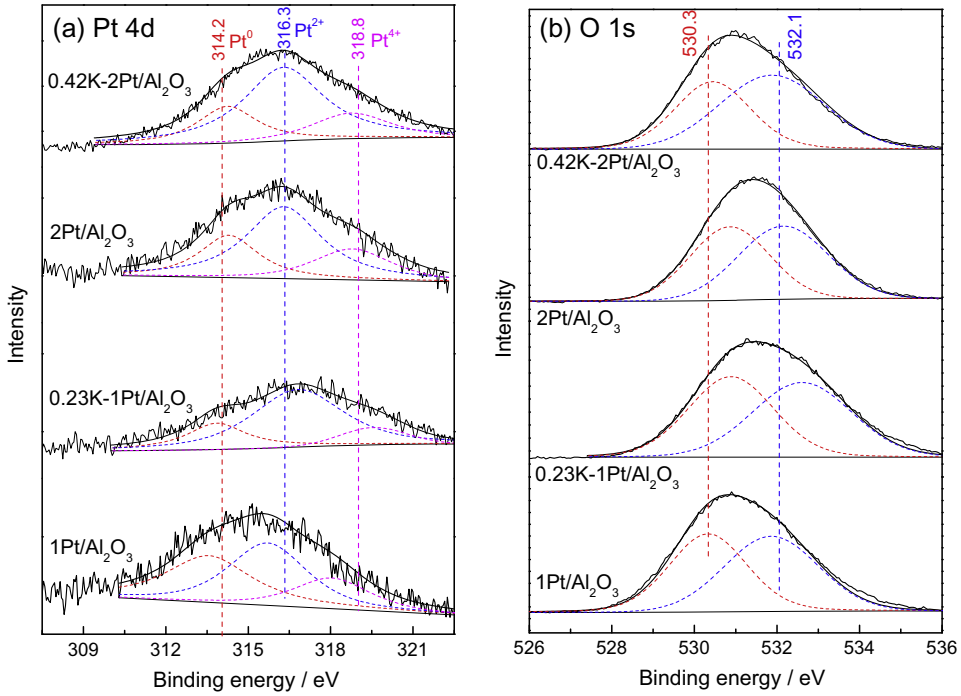

Fig. 5. (a) Pt4d and (b) O1s XPS spectra of $1Pt/Al_2O_3$, $0.23K–1Pt/Al_2O_3$, $2Pt/Al_2O_3$ and $0.42K–2Pt/Al_2O_3$ catalysts.

Table 2
Binding energies and surface compositions of Pt and O species in catalysts.

Catalyst	Pt $4d_{5/2}$/eV (molar content/%)			O 1s/eV (molar content/%)	
	Pt^0	Pt^{2+}	Pt^{4+}	O_{latt}	O_{ads}
$1Pt/Al_2O_3$	313.6 (37.4)	316.2 (49.2)	319.1 (13.4)	530.3 (47.4)	531.9 (52.6)
$0.23K–1Pt/Al_2O_3$	313.8 (20.7)	316.3 (60.4)	319.2 (18.9)	530.9 (48.8)	532.6 (51.2)
$2Pt/Al_2O_3$	314.3 (24.5)	316.3 (53.9)	318.8 (21.6)	530.9 (47.4)	532.2 (52.6)
$0.42K–2Pt/Al_2O_3$	314.2 (21.9)	316.3 (60.2)	318.7 (17.9)	530.5 (39.5)	531.8 (60.5)

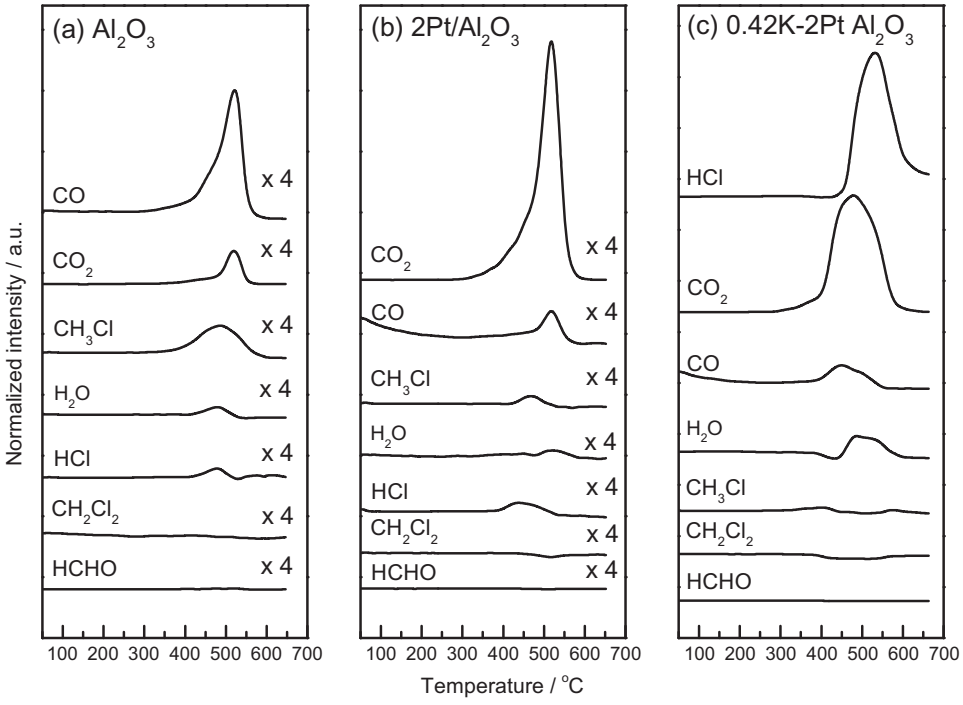

Fig. 6. MS signals of various products over (a) Al_2O_3, (b) $2Pt/Al_2O_3$ and (c) $0.42K–2Pt/Al_2O_3$ catalysts.

HCl. Other intermediates such as HCHO are not detected. The formation of CO, CH_3Cl and HCl is due to the disproportionation of CH_2Cl_2 on Al_2O_3 [48], while the CO_2 and H_2O products could be formed by further reaction between $CO + O_2$ and $CH_3Cl + O_2$, respectively. On the $2Pt/Al_2O_3$ catalyst (Fig. 6b), the products are similar to those obtained on the Al_2O_3, but obvious difference is also observed. The formation of CO_2 becomes dominant, accompanied by the dramatic reduction of CO and CH_3Cl formation. This comparison indicates that the presence of Pt species in the catalyst remarkably accelerates the oxidation reaction, particularly the CO oxidation ($2CO + O_2 \rightarrow 2CO_2$), which is understandable because Pt is very active for CO oxidation [49]. These results are also in good agreement with the literature. For example, Maupin et al. [48] proposed a bifunctional mechanism for CH_2Cl_2 oxidation over Pt/Al_2O_3 catalysts, that is, CH_2Cl_2 disproportionation over Al_2O_3 and oxidation over Pt. With the K-promotion (Fig. 6c), the oxidation of CH_2Cl_2 is even more pronounced, judging from the intensities of the products (note that the product intensities are magnified by 4 in Fig. 6a and b). These results clearly indicate that the activity could be remarkably enhanced on the $0.42K–2Pt/Al_2O_3$ catalyst.

Then, CH_2Cl_2 oxidation was carried out in a conventional fixed-bed reactor over various Pt/Al_2O_3 catalysts (Fig. 7). For the $0.1Pt/Al_2O_3$ catalyst, the promotion of K slightly improves the activity, as the $0.1Pt/Al_2O_3$ and $0.02K–0.1Pt/Al_2O_3$ catalysts essentially have almost identical catalytic performance at low-temperature region but the latter catalyst is slightly more active than the former at reaction temperature higher than 370 °C (Fig. 7a). With increasing Pt content in the catalyst, the promoting effect of K becomes significant (Fig. 7b–d). For example, a full conversion of CH_2Cl_2 is obtained at about 500 °C on the $1Pt/Al_2O_3$, while on the K-promoted sample ($0.23K–1Pt/Al_2O_3$) the full conversion of CH_2Cl_2 is achieved at 365 °C, which is 135 °C lower than on the $1Pt/Al_2O_3$ (Fig. 7c).

To better illustrate the remarkable enhancement of activity by K-promotion, comparison of T_{50} values of the catalysts (the reaction temperature at which the CH_2Cl_2 conversion is 50%) was made based on the results in Fig. 7. As shown in Fig. 8, it is clear that the T_{50} values are quite close (380–402 °C) for the K-free samples. These results imply that for the Pt/Al_2O_3 catalysts, the activities are not affected by Pt content and Pt particle size, which is consistent with the previous report [48]. However, the K-promotion in the catalyst lowers the T_{50} values. Interestingly, the difference in T_{50} values between the K-promoted and the K-free counterpart becomes more pronounced with increasing Pt content in the catalyst. The lowest T_{50} is obtained on the $0.42K–2Pt/Al_2O_3$ catalyst (270 °C), which is much lower than that on the $2Pt/Al_2O_3$ (402 °C).

Also, catalyst stability was also investigated on the $0.42K–2Pt/Al_2O_3$ catalyst at the reaction temperature of 320 °C. As can be seen in Fig. 9, the catalyst is quite stable, with a CH_2Cl_2 conversion of about 90% during the reaction period (10 h).

4. Discussion

In this work, remarkably enhancement of CH_2Cl_2 oxidation was found over the K-promoted Pt/Al_2O_3 catalysts. These catalysts are more active than the CeO_2-modified Pt/Al_2O_3 catalysts for CH_2Cl_2 oxidation under identical reaction conditions as reported in our previous work [31]. For example, the T_{50} value on a 2.0Pt/15CeAlO catalyst was 317 °C, which is almost 50 °C higher than that on the $0.42K–2Pt/Al_2O_3$ in the current work. Therefore, the relationship between the catalyst natures and their catalytic behaviors deserves a detailed discussion.

Turnover frequencies of the catalysts based on Pt dispersion are calculated and listed in Table 1. For either series of K-free or K-promoted Pt/Al_2O_3 catalysts, it is found that the TOF decreases with increasing Pt content in the catalyst, which has been observed in our previous work on the Pt/CeAlO catalysts [31]. Since it is known that for the Pt/Al_2O_3 catalysts, the activities are not affected by Pt content and Pt particle size as previously reported [48] and in the current work (Figs. 7 and 8), such comparison of the TOFs might not give reliable information on the intrinsic activities of

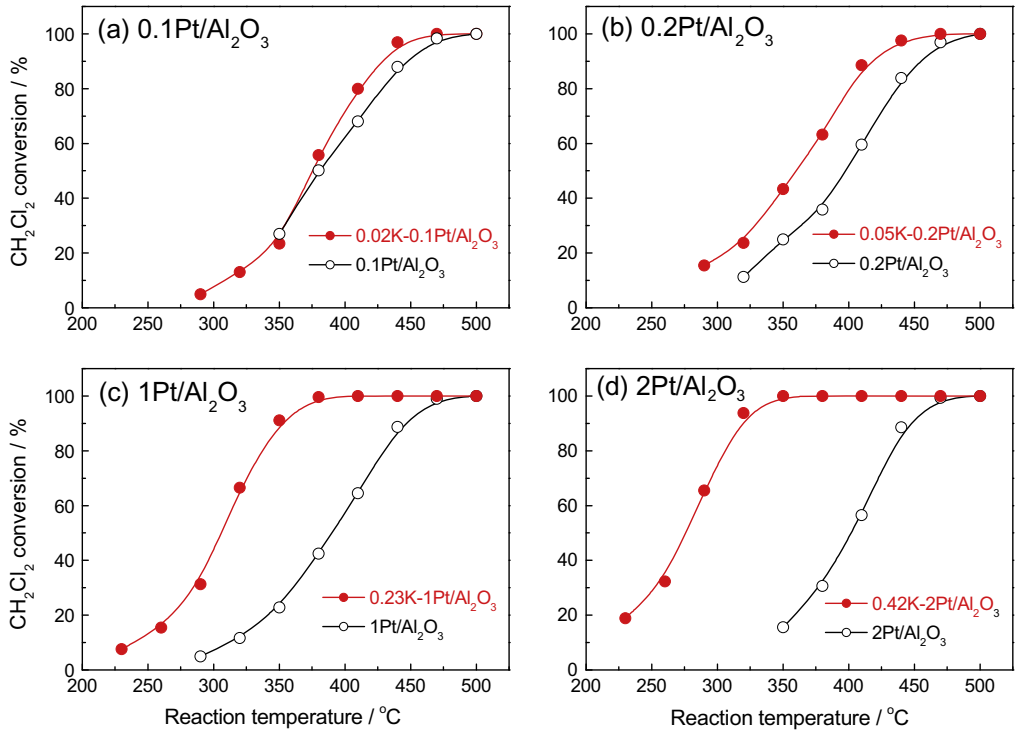

Fig. 7. Comparison of catalytic performance of Pt/Al_2O_3 catalysts with or without K-promotion.

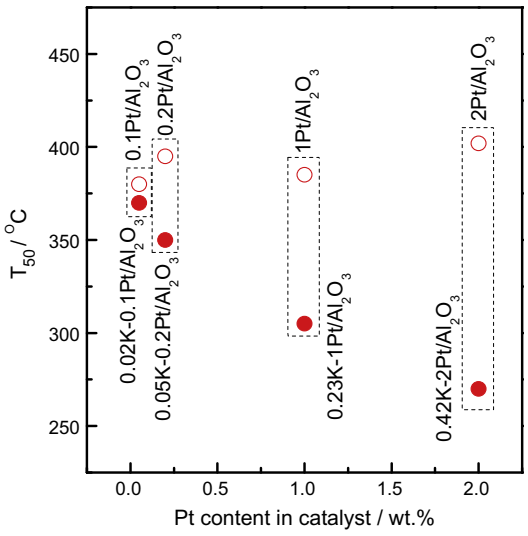

Fig. 8. Comparison of T_{50} temperatures of various Pt/Al_2O_3 catalysts.

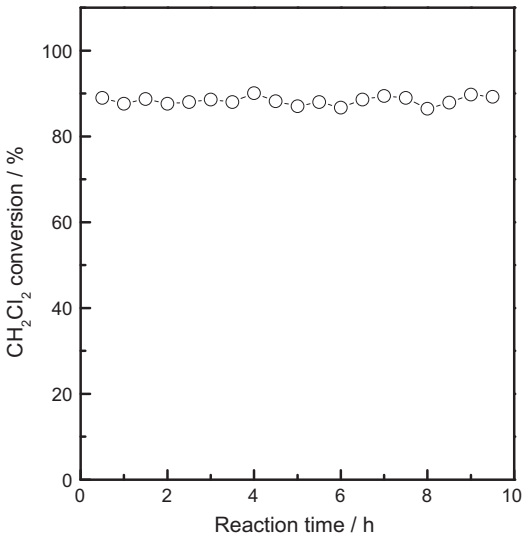

Fig. 9. Stability of 0.42K–2Pt/Al_2O_3 catalyst at reaction temperature of 320 °C.

the catalysts. Nevertheless, the comparison of the TOFs between the K-promoted catalyst and the corresponding K-free one could still reflect the promoting effect of K. It is found that the TOF of the K-promoted sample is higher than the corresponding K-free one, particularly for those with high Pt loadings (Pt content >1 wt.%). For example, the TOF on the 0.42K–2Pt/Al_2O_3 is 1.81×10^{-2} s^{-1} at 350 °C, which is almost 5-fold as high as that on the 2Pt/Al_2O_3 (0.37×10^{-2} s^{-1}). These results again confirm the remarkable enhancement of catalytic activity by the K-promotion.

In the current work, the first thing to be mentioned is the washing process during the catalyst preparation. In the reported works on water–gas-shift reaction [37] and HCHO oxidation [39], the alkali-modified catalysts had identical activities with or without washing. However, the situation is completely different in the current work. A catalyst containing 1.0 wt.% of K was prepared by an incipient wetness impregnation method without washing (1K–2Pt/Al_2O_3) and tested for CH_2Cl_2 oxidation. It is found that its activity is close to that of the K-free 2Pt/Al_2O_3 catalyst (Fig. 10). Then, the1K–2Pt/Al_2O_3 was washed for three times with deionized water and its K content became 0.42 wt.%. The reduced K content in

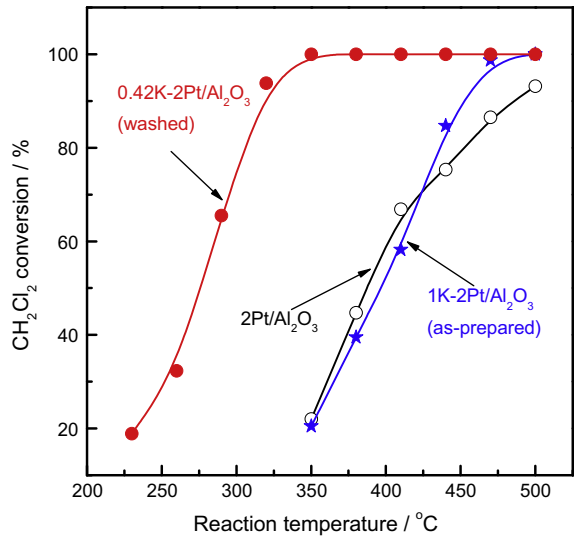

Fig. 10. Effect of catalyst washing on the catalytic performance.

the catalyst after the washing is due to the fact that the potassium salt could be dissolved in water and be removed from the catalyst. The resulting catalyst (0.42K–2Pt/Al_2O_3) shows remarkable improvement in activity. This comparison suggests that excessive K species in the catalyst could possibly block some active sites for the reaction, which are most likely the acidic sites on Al_2O_3 since these sites are centers for CH_2Cl_2 chemisorption [50].

To explain the remarkable activities on the K–Pt/Al_2O_3 catalysts, we first consider the possibility of the changes of reaction pathways on these catalysts. Thus, kinetic studies were performed on the 2Pt/Al_2O_3 and 0.42K–2Pt/Al_2O_3 catalysts and the Arrhenius plots are shown in Fig. 11. Note that the CH_2Cl_2 conversions are low (typically less than 15%) to ensure a differential reaction mode on the catalyst (see Table S1 in Supplementary information for detailed results of conversions and reaction rates). It is found that the apparent activation energies obtained on these two catalysts are essentially same (129.4 kJ mol^{-1} for the 2Pt/Al_2O_3 and 115.5 kJ mol^{-1} for the 0.42K–2Pt/Al_2O_3), suggesting that the reaction pathway does not change after the K-promotion.

Surface acidity and catalyst reducibility are two important parameters for CVOCs oxidation, and the activity of the catalyst is usually determined by synergetic effects of these two

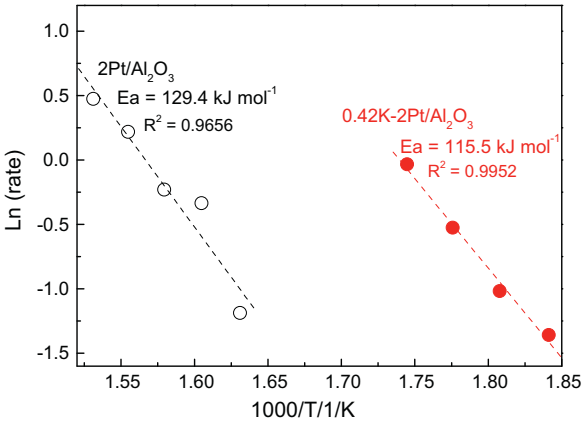

Fig. 11. Arrhenius plots of CH_2Cl_2 oxidation over 2Pt/Al_2O_3 and 0.42K–2Pt/Al_2O_3 catalysts.

parameters [17,31]. Our findings reveal that blockage of surface acidic sites leads to the suppression of activity (Fig. 10) and the K-free Pt/Al_2O_3 catalysts have higher surface acidity than the K-modified samples (Fig. 4), then it appears that redox properties of the catalysts play very important role in the reaction. In the current work, the H_2-TPR results (Fig. 3) show that enhanced reducibility is observed on the K-promoted catalysts (particularly on the 0.23K–1Pt/Al_2O_3 and 0.42K–2Pt/Al_2O_3). Although the influence of decreased Pt particle sizes in the K-promoted samples on the catalyst reducibility cannot be ruled out, such an enhancement is possibly related to the presence of K species in the catalysts. Also, as the catalysts were subjected to a washing procedure, the remaining K species in the catalysts are likely in contact with the Pt entities (because the K species contact with Al_2O_3 could be easily removed by washing), which is hinted by the fact that the K contents change with the Pt contents in the catalysts (Table 1) and the K/Pt ratio in these catalysts are close to 1. Note that the K/Pt ratios of 1 in these samples refer to the bulk composition and the particle sizes of Pt in the catalysts are essentially about 2 nm (Table 1), which corresponds to surface K/Pt ratios close to 2 if we assume that the K species are all isolated ions. Such surface Pt–O–K_x ($x \approx 2$) species generated by the interaction between K and Pt may be responsible for the promoted catalyst reducibility and consequently the activity. Although the exact geometry of these Pt–O–K_x species is not clear, their promoting effects in catalyst reducibility have been reported in a recent work. Zhai et al. [37] reported a very active 1Pt–3Na–SiO_2 catalyst with a surface Na/Pt ratio of 3 for water–gas-shift reaction. The authors also found that the alkali ions introduced reducible surface oxygen and stated that the activity of the reaction was associated with the Pt–O_x–Na species, as evidenced by the CO-TPR results.

In order to further understand the catalytic behaviors of the catalysts, in situ FTIR experiments were conducted on the Al_2O_3, 2Pt/Al_2O_3 and 0.42K–2Pt/Al_2O_3 catalysts and the results are shown in Fig. 12. For the Al_2O_3 support (Fig. 12a), after the introduction of CH_2Cl_2 and O_2, the IR spectra show bands at 1373, 1390, 1588, 1630, 2985, 3010 and 3673 cm^{-1}. According to literature [48], the broad band at 3673 cm^{-1} is assigned to hydroxyl groups (–OH) in Al_2O_3 and the band at 1630 cm^{-1} is assigned to adsorbed H_2O. The band at 3010 cm^{-1} is assigned to gas-phase CH_2Cl_2 while the band at 2985 cm^{-1} is assigned to CH_2Cl_2 adsorbed on Al_2O_3. The bands at 1588 and 1373 cm^{-1} are due to asymmetric and symmetric vibrations of formate species (–COOH), while the band at 1390 cm^{-1} corresponds to C–H displacement of formate species. At elevated temperature, the intensity of the band at 1588 cm^{-1} progressively increases, but other bands keep almost constant. The CH_2Cl_2 oxidation over Al_2O_3 was investigated in detail in previous works and formate species are found to be intermediates during the reaction [48,51]. The increasing intensity of the formate species implies that more CH_2Cl_2 molecules are consumed at elevated temperatures. When the reaction was performed on the 2Pt/Al_2O_3 catalyst (Fig. 12b), similar bands are observed as on the Al_2O_3 support but the band at 1588 cm^{-1} is much less intense on this catalyst. Moreover, a very weak band at 2126 cm^{-1} is observed at 100 °C, which could be assigned to CO chemisorbed on oxidized Pt^{2+} sites [52–54]. This band (2126 cm^{-1}) is also accompanied by the emergence of a broad band at 2360 cm^{-1}, which is assigned to gas-phase CO_2. The IR spectra on the 0.42K–2Pt/Al_2O_3 (Fig. 12c) contain essentially similar features as those on the 2Pt/Al_2O_3, except that the intensity of the band at 2126 cm^{-1} is stronger.

To conveniently compare the IR results on these three catalysts, normalized intensities of the characteristic bands at 1588 and 2126 cm^{-1} as a function of temperature were plotted and shown in Fig. 13. For the intensity of formate species (Fig. 13a), it is found that it is much higher on the Al_2O_3 than on the 2Pt/Al_2O_3 or 0.42K–2Pt/Al_2O_3. While for the chemisorbed CO, its intensity is higher on the 0.42K–2Pt/Al_2O_3 than on the 2Pt/Al_2O_3, but no signal of this band is detected on Al_2O_3 because of the absence of Pt.

The reaction of CH_2Cl_2 over Al_2O_3 was investigated in literature [48]. CH_2Cl_2 molecules first disproportionate on the surface to produce HCl and a chloromethoxyl specie, followed by chloromethoxy dismutation to form CH_3Cl and formate species. Finally, the formate species could be decomposed to CO. Thus, the overall reaction of CH_2Cl_2 over Al_2O_3 could be written as the following the equation:

$$2CH_2Cl_2 + H_2O \rightarrow CO + CH_3Cl + 3HCl$$

This reaction pathway is in good accordance with the TPSR results (Fig. 6), as the main products obtained on the Al_2O_3 support are CO and CH_3Cl. Also, the formation of the formate species on Al_2O_3 is confirmed by the IR results (Figs. 12a and 13). With the presence of Pt in the catalyst, the formate species could be decomposed to CO and chemisorbed on Pt entities (Figs. 12b and c and 13), which could further react with oxygen species on Pt to produce CO_2, following a bifunctional mechanism proposed by Maupin et al. [48] and Pinard et al. [55] (CH_2Cl_2 disproportionation on Al_2O_3 and oxidation over Pt), as evidenced in Fig. 6 that on the 2Pt/Al_2O_3 and 0.42K–2Pt/Al_2O_3 catalysts the main products are CO_2. Moreover, the intensity of the formate species on the 0.42K–2Pt/Al_2O_3 catalyst is lower compared to that on the 2Pt/Al_2O_3 (Fig. 13), suggesting that the K-promotion in the Pt/Al_2O_3 catalyst leads to more pronounced decomposition of the formate species. Such enhanced decomposition of formate species on alkali-promoted Pt catalysts was also reported in literature. Evin et al. [56] found that the formate decomposition rates were higher on Li- and Na-promoted Pt/CeO_2 catalysts compared to a bare Pt/CeO_2. Interestingly, this finding is also consistent with the observation of HCHO oxidation over Pt/TiO_2 catalysts. It was reported that formate species are intermediates in HCHO oxidation over Pt/TiO_2 catalysts [57], which could further decompose to CO by the reaction HCOO-M → CO-M + OH-M. The chemisorbed CO (CO-M) could subsequently reaction with oxygen to form CO_2. The same group [39] recently reported that alkali metal-promoted Pt/TiO_2 catalysts (alkali metal = Li, Na or K) had superior activity for HCHO reaction compared to the alkali metal-free Pt/TiO_2 catalyst. The authors concluded that the enhancement of the activity was due to the presence of Pt–$O(OH)_x$-alkali-metal species which could alter the reaction pathway from HCOO-M → CO-M + OH-M to HCOO-M + OH-M → CO_2 + H_2O + 2 M. In our case, since the apparent energies of the CH_2Cl_2 oxidation over the 2Pt/Al_2O_3 and 0.42K–2Pt/Al_2O_3 catalysts are similar (Fig. 11) and changes in the hydroxyl groups are difficult to analyze because of the broad region of this group in IR spectra (Fig. 12), no concrete conclusion on the mechanistic insights for this reaction could be made. Nevertheless, one remark on the catalytic behaviors of these catalysts could be reached, that is, the decomposition of formate intermediate could be remarkably accelerated over the K-promoted sample, as shown in Figs. 12 and 13. Moreover, since the overall activity of the 0.42K–2Pt/Al_2O_3 catalyst is much higher than that on the 2Pt/Al_2O_3, it implies that the decomposition of the formate species might be the rate determining step for the CH_2Cl_2 oxidation.

Therefore, in the current case, it appears that the improved activities on the K-promoted Pt/Al_2O_3 catalysts are due the enhanced catalyst reducibility induced by the generation of surface Pt–O–K_x species, which could accelerate the decomposition of formate species to CO and thus shift the reaction equilibrium. In addition, as the activity depends on such species, it well explains the best performance on the 0.42K–2Pt/Al_2O_3 compared to the others, because it contains the highest amount of the Pt–O–K_x species.

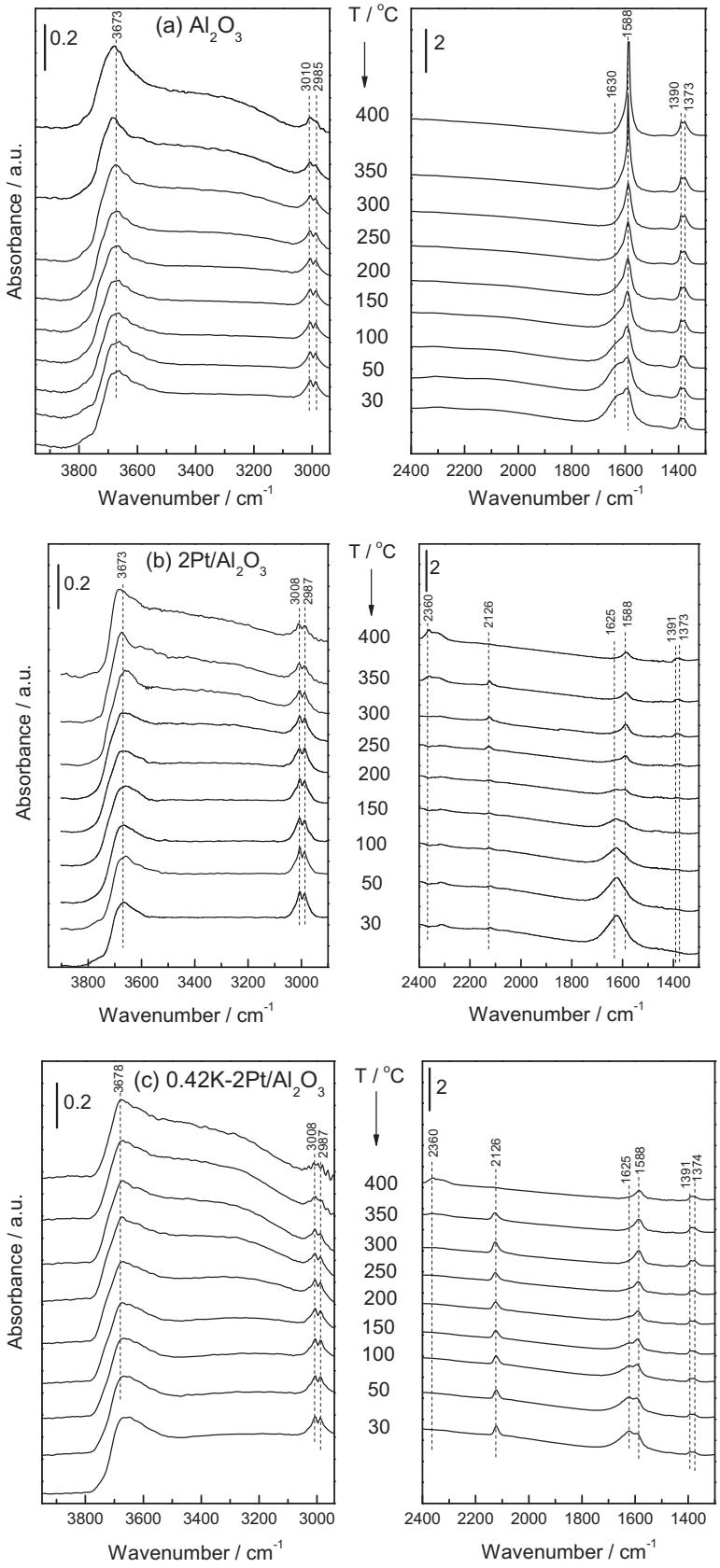

Fig. 12. In situ FTIR spectra of surface reaction of $CH_2Cl_2 + O_2$ over (a) Al_2O_3, (b) $2Pt/Al_2O_3$ and (c) $0.42K–2Pt/Al_2O_3$ catalysts.

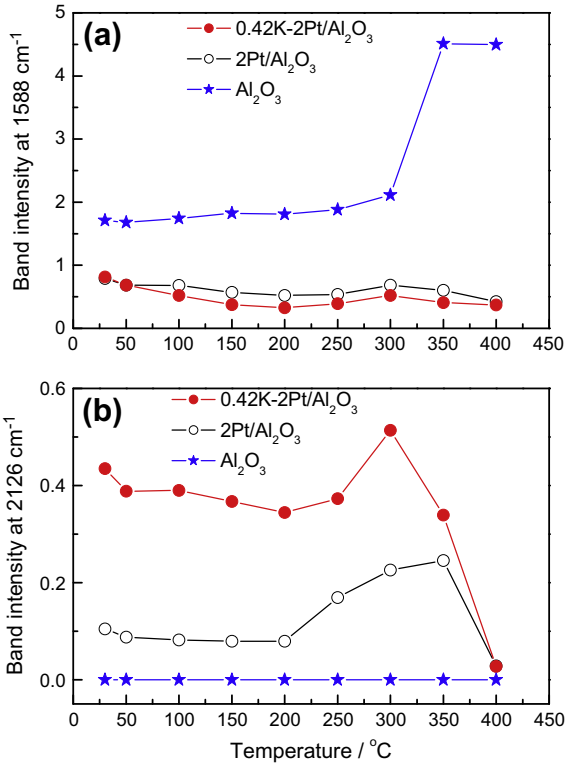

Fig. 13. Intensity of characteristic bands as a function of temperature over different catalysts. (a) Band at 1588 cm^{-1} (formate species); (b) band at 2126 cm^{-1} (chemisorbed CO).

5. Conclusion

This work demonstrates the remarkable enhancement of activity for CH_2Cl_2 oxidation over Pt/Al_2O_3 catalysts with the alkali metal promotion. Introduction of K in the catalyst leads to the generation of Pt–O–K_x species induced by an interaction between K and Pt. These species have enhanced reducibility and accelerate the decomposition of formate intermediates in the reaction, and thus promote the overall activity.

Acknowledgments

This work is financially supported by the Natural Science Foundation of China (Grant No. 21173195) and the Public Welfare Program of Science Technology Department of Zhejiang Province (Grant No. 2013C31049).

Appendix A. Supplementary material

Supplementary data associated with this article can be found, in the online version, at http://dx.doi.org/10.1016/j.jcat.2013.12.018.

References

[1] S. Reimann, A.C. Lewis, in: R. Koppmann (Ed.), Volatile Organic Compounds in the Atmosphere, Blackwell Publishing Ltd., Oxford, 2007.
[2] K. Everaert, J. Baeyens, J. Hazard. Mater. 109 (2004) 113.
[3] L.F. Wang, M. Sakurai, H. Kameyama, J. Hazard. Mater. 154 (2008) 390.
[4] S. Pitkäaho, L. Matejova, S. Ojala, J. Gaalova, R.L. Keiski, Appl. Catal. B: Environ. 113 (2012) 150.
[5] A. Musialik-Piotrowska, Catal. Today 119 (2007) 301.
[6] H. Windawi, Z.C. Zhang, Catal. Today 30 (1996) 99.
[7] J.C. Lou, S.S. Lee, Appl. Catal. B: Environ. 12 (1997) 111.
[8] Q. Dai, X. Wang, G. Lu, Appl. Catal. B: Environ. 81 (2008) 192.
[9] G. Sinquin, C. Petit, S. Libs, J.P. Hindermann, A. Kiennemann, Appl. Catal. B: Environ. 27 (2000) 105.
[10] S.D. Yim, K.H. Chang, D.J. Koh, I.S. Nam, Y.G. Kim, Catal. Today 63 (2000) 215.
[11] F. Solymosi, J. Raskó, E. Papp, A. Oszkó, T. Bánsági, Appl. Catal. A: Gen. 131 (1995) 55.
[12] V. Szabo, M. Bassir, A. Van Neste, S. Kaliaguine, Appl. Catal. B: Environ. 37 (2002) 175.
[13] N.A. Merino, B.P. Barbero, P. Grange, L.E. Cadus, J. Catal. 231 (2005) 232.
[14] Y. Liu, H. Dai, Y. Du, J. Deng, L. Zhang, Z. Zhao, C.T. Au, J. Catal. 287 (2012) 149.
[15] A. Aranzabala, J.A. González-Marcosa, M. Romero-Sáez, J.R. González-Velasco, M. Guillemot, P. Magnoux, Appl. Catal. B: Environ. 88 (2009) 533.
[16] J.R. González-Velasco, R. López-Fonseca, A. Aranzabal, J.I. Gutiérrez-Ortiz, P. Steltenpohl, Appl. Catal. B: Environ. 24 (2000) 233.
[17] Q. Huang, X. Xue, R. Zhou, J. Hazard. Mater. 183 (2010) 694.
[18] A. Aranzabal, J.A. González-Marcosa, M. Romero-Sáez, J.R. González-Velasco, M. Guillemot, P. Magnoux, Appl. Catal. B: Environ. 88 (2009) 533.
[19] R. Rachapudi, P.S. Chintawar, H.L. Greene, J. Catal. 185 (1999) 58.
[20] I.M. Freidel, A.C. Frost, K.J. Herbert, F.S. Meyer, J.C. Summers, Catal. Today 17 (1993) 367.
[21] B. de Rivas, R. López-Fonseca, C. Sampedro, J.I. Gutiérrez-Ortiz, Appl. Catal. B: Environ. 90 (2009) 545.
[22] B. de Rivas, López-Fonseca, M. Gutiérrez-Ortiz, J.I. Gutiérrez-Ortiz, Appl. Catal. B: Environ. 101 (2011) 317.
[23] A. Parinyaswan, S. Pongstabodee, A. Luengnaruemitchai, J. Hydrogen Energy 31 (2006) 1942.
[24] P. Djinovic, J. Levec, A. Pintar, Catal. Today 138 (2008) 222.
[25] X.Y. Wang, Q. Kang, D. Li, Appl. Catal. B: Environ. 86 (2009) 166.
[26] Q.Q. Huang, Z.H. Meng, R.X. Zhou, Appl. Catal. B: Environ. 115–116 (2012) 179.
[27] C. Zhang, W. Hua, C. Wang, Y. Guo, Y. Guo, G. Lu, A. Baylet, A. Giroir-Fendler, Appl. Catal. B: Environ. 134–135 (2013) 310.
[28] D.M. Papenmeier, J.A. Rossin, Ind. Eng. Chem. Res. 33 (1994) 3094.
[29] B. Miranda, E. Díaz, S. Ordónez, A. Vega, F.V. Díez, Chemosphere 66 (2007) 1706.
[30] S. Pitkäaho, S. Ojalaa, T. Maunulab, A. Savimäkib, T. Kinnunenb, R.L. Keiski, Appl. Catal. B: Environ. 102 (2011) 395.
[31] Q.Y. Chen, N. Li, M.F. Luo, J.Q. Lu, Appl. Catal. B: Environ. 127 (2012) 159.
[32] Z. Abbasi, M. Haghighi, E. Faterhifar, S. Saedy, J. Hazard. Mater. 186 (2011) 1445.
[33] M. Kuriyama, H. Tanaka, S. Ito, T. Kubota, T. Miyao, S. Naito, K. Tomishige, K. Kunimori, J. Catal. 252 (2007) 39.
[34] Y. Minemura, M. Kuriyama, S. Ito, K. Tomishige, K. Kunimori, Catal. Commun. 7 (2006) 623.
[35] X. Yu, W. Yu, H. Li, S.T. Tu, Y.F. Han, Appl. Catal. B: Environ. 140–141 (2013) 588.
[36] X. Zhu, T. Hoang, L. Lobban, R. Mallinson, Catal. Lett. 129 (2009) 135.
[37] Y. Zhai, D. Pierre, R. Si, W. Deng, P. Ferrin, A.U. Nilekar, G. Peng, J.A. Herron, D.C. Bell, H. Saltsburg, M. Mavrikakis, M. Flytzani-Stephanopoulos, Science 329 (2010) 1633.
[38] J.M. Pigos, C.J. Brooks, G. Jacobs, B.H. Davis, Appl. Catal. A Gen. 319 (2007) 47.
[39] C. Zhang, F. Liu, Y. Zhai, H. Ariga, N. Yi, Y. Liu, K. Asakura, M. Flytzani-Stephanopoulos, H. He, Angew. Chem. Int. Ed. 51 (2012) 9628.
[40] H.S. Fogler, Elements of Chemical Reaction Engineering, Pearson Education Inc., forth ed., 2006, p. 839.
[41] S. Jongpatiwut, N. Rattanapuchapong, T. Rirksomboon, S. Osuwan, D.E. Resasco, Catal. Lett. 122 (2008) 214.
[42] M. Paulis, H. Peyrard, M. Montes, J. Catal. 199 (2001) 30.
[43] M. García-Dieguez, I.S. Pieta, M.C. Herrera, M.A. Larrubia, I. Malpartida, L.J. Alemany, Catal. Today 149 (2010) 380.
[44] G. Corro, C. Cano, J.L.G. Fierro, J. Mol. Catal. A: Chem. 315 (2010) 35.
[45] M.J. Tiernan, O.E. Finlayson, Appl. Catal. B: Environ. 19 (1998) 23.
[46] I. Tankov, K. Arishtirova, J.M.C. Bueno, S. Damyanova, Appl. Catal. A: Gen. (2013), http://dx.doi.org/10.1016/j.apcata.2013.08.030.
[47] A. Machocki, T. Ioannides, B. Stasinska, W. Gac, G. Avgouropoulos, D. Delimaris, W. Grzegorczyk, S. Pasieczna, J. Catal. 227 (2004) 282.
[48] I. Maupin, L. Pinard, J. Mijion, P. Magnoux, J. Catal. 291 (2012) 104.
[49] A.D. Allian, K. Takanabe, K.L. Fujdala, X. Hao, T.J. Truex, J. Cai, C. Buda, M. Neurock, E. Iglesia, J. Am. Chem. Soc. 133 (2011) 4498.
[50] L. Intriago, E. Díaz, S. Ordóñez, A. Vega, Microporous Mesoporous Mater. 91 (2006) 161.
[51] R.W. van den Brink, P. Mulder, R. Louw, G. Sinquin, C. Petit, J.P. Hindermann, J. Catal. 180 (1998) 153.
[52] P. Panagiotopoulou, A. Christodoulakis, D.I. Kondarides, S. Boghosian, J. Catal. 240 (2006) 114.
[53] P.A. Carlsson, L. österlund, P. Thormählen, A. Palmqvist, E. Fridell, J. Jansson, M. Skoglundh, J. Catal. 226 (2004) 422.
[54] N. Li, Q.Y. Chen, L.F. Luo, W.X. Huang, M.F. Luo, G.S. Hu, J.Q. Lu, Appl. Catal. B: Environ. 142–143 (2013) 523.
[55] L. Pinard, J. Mijoin, P. Magnoux, M. Guisnet, J. Catal. 215 (2003) 234.
[56] H.N. Evin, G. Jacobs, J. Ruiz-Martinez, U.M. Graham, A. Dozier, G. Thomas, B.H. Davis, Catal. Lett. 122 (2008) 9.
[57] C. Zhang, H. He, K. Tanaka, Appl. Catal. B: Environ. 65 (2006) 37.